AGU PUBLICATIONS

JGR

Journal of Geophysical Research: Oceans

RESEARCH ARTICLE

10.1002/2013JC009385

Key Points:
- Alongshore wind modulates advective processes along the Northwest Atlantic shelf
- Wind offers a viable mechanism to explain interannual salinity patterns in GoM

Correspondence to:
Y. Li,
yli@whoi.edu

Citation:
Li, Y., R. Ji, P. S. Fratantoni, C. Chen, J. A. Hare, C. S. Davis, and R. C. Beardsley (2014), Wind-induced interannual variability of sea level slope, along-shelf flow, and surface salinity on the Northwest Atlantic shelf, *J. Geophys. Res. Oceans*, *119*, 2462–2479, doi:10.1002/2013JC009385.

Received 29 AUG 2013
Accepted 21 MAR 2014
Accepted article online 25 MAR 2014
Published online 16 APR 2014

Wind-induced interannual variability of sea level slope, along-shelf flow, and surface salinity on the Northwest Atlantic shelf

Yun Li[1,2], Rubao Ji[2], Paula S. Fratantoni[3], Changsheng Chen[4], Jonathan A. Hare[3], Cabell S. Davis[2], and Robert C. Beardsley[5]

[1]Integrated Statistics under Contract with NOAA NMFS, Northeast Fisheries Science Center, Woods Hole, Massachusetts, USA, [2]Department of Biology, Woods Hole Oceanographic Institution, Woods Hole, Massachusetts, USA, [3]NOAA NMFS, Northeast Fisheries Science Center, Woods Hole, Massachusetts, USA, [4]School for Marine Science and Technology, University of Massachusetts–Dartmouth, New Bedford, Massachusetts, USA, [5]Department of Physical Oceanography, Woods Hole Oceanographic Institution, Woods Hole, Massachusetts, USA

Abstract In this study, we examine the importance of regional wind forcing in modulating advective processes and hydrographic properties along the Northwest Atlantic shelf, with a focus on the Nova Scotian Shelf (NSS)-Gulf of Maine (GoM) region. Long-term observational data of alongshore wind stress, sea level slope, and along-shelf flow are analyzed to quantify the relationship between wind forcing and hydrodynamic responses on interannual time scales. Additionally, a simplified momentum balance model is used to examine the underlying mechanisms. Our results show significant correlation among the observed interannual variability of sea level slope, along-shelf flow, and alongshore wind stress in the NSS-GoM region. A mechanism is suggested to elucidate the role of wind in modulating the sea level slope and along-shelf flow: stronger southwesterly (northeastward) winds tend to weaken the prevailing southwestward flow over the shelf, building sea level in the upstream Newfoundland Shelf region, whereas weaker southwesterly winds allow stronger southwestward flow to develop, raising sea level in the GoM region. The wind-induced flow variability can influence the transport of low-salinity water from the Gulf of St. Lawrence to the GoM, explaining interannual variations in surface salinity distributions within the region. Hence, our results offer a viable mechanism, besides the freshening of remote upstream sources, to explain interannual patterns of freshening in the GoM.

1. Introduction

A dominant feature of the hydrography on the Northwest Atlantic shelf is the prevalence of relatively cold and fresh coastal-trapped waters flowing equatorward [*Loder et al*., 1998a, 1998b], having freshwater sources derived from high latitudes [*Chapman et al*., 1986; *Chapman and Beardsley*, 1989]. On the Nova Scotian Shelf (NSS), the Scotia Shelf Current (SSC) is an inshore branch of this southwestward flow that is fed by a mixture of waters from the Labrador Shelf and Gulf of St. Lawrence (GSL) [*Houghton and Fairbanks*, 2001] (see Figure 1 for locations). The SSC transports the colder and fresher Scotian Shelf Water (SSW) into the Gulf of Maine (GoM) within the surface layer (upper 100 m), with one branch entering around Cape Sable inshore of Browns Bank [*Smith*, 1983, 1989; *Brown and Irish*, 1993] and another entering offshore of Browns Bank via the Northeast Channel [*Smith*, 1983, 1989].

The NSS-GoM region lies within an extended boundary current system characterized by variable transport, driven by both wind stress and thermohaline forcings, and large hydrographic variability. *Petrie and Drinkwater* [1993] describe interannual fluctuations in temperature and salinity over the period 1945–1990 reaching 4.63°C and 0.7, respectively, concluding that these variations are associated with variations in the Labrador Current transport. *Loder et al*. [2001] use historical data (1900–2000) and a circulation model to demonstrate that decadal-scale hydrographic variations are common in the NSS-GoM region. While there is a growing interest in hydrographic variability within the broader interdisciplinary community, the mechanisms behind these large changes are poorly understood, limiting our ability to develop indices for prediction.

The hydrographic conditions in the GoM are largely determined by the relative proportion of two main sources of water entering the region: cold, fresh SSW advected southwestward along the shelf and warm, saline slope waters residing offshore of the shelf break. The hydrographic properties and volume of these

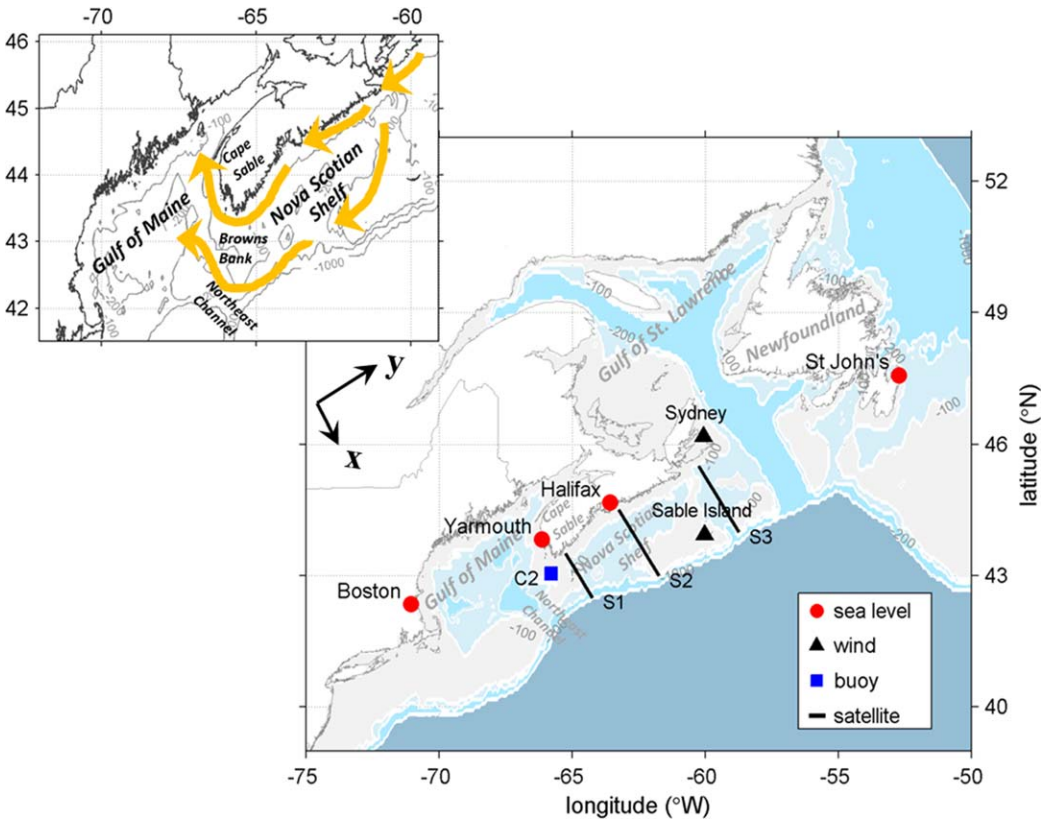

Figure 1. Bathymetric features of the Nova Scotian Shelf (NSS) and adjacent regions. The contours show water depth in meters. Red dots correspond to long-term tide gauges. Black triangles represent long-term wind stations. The blue square shows the GLOBEC Cape Sable mooring (C2) which lies on the 110 m isobath, and the black lines denote the three cross-shelf transects used in the subsequent analysis of altimetry data. The inset shows the schematic diagram of the Scotian Shelf Current (SSC) and its inshore and offshore branches that enter the Gulf of Maine (GoM).

source waters exhibit significant low-frequency (longer than 1 year) variability. For example, the inflow of SSW was stronger and surface salinity was lower during the 1990s than during the mid-late 1970s [*Smith et al.*, 2001]. While the total volume transport entering the GoM was fairly constant, the volumetric inflow of SSW was nearly doubled during the mid-1990s, as revealed by current measurements from a mooring deployed during the Georges Bank GLOBEC (Global Ocean Ecosystem Dynamics) program [*Smith et al.*, 2001]. Due to the increase in the inflow of low-salinity waters from the NSS and a coincident decrease in the inflow of warm, saline slope water through the Northeast Channel [*Smith et al.*, 2012], surface waters (0–30 m) in the interior GoM were markedly fresher during this period [*Mountain*, 2004].

Given the observational evidence that salinity variability in the NSS-GoM region may be linked to large changes in nutrient loading and food-web dynamics on the shelf [i.e., *Loder et al.*, 2001; *Townsend et al.*, 2010], efforts have been made to identify mechanisms that would drive oscillations in hydrographic properties, focusing in particular on changes in the volume or property of remote upstream sources [*Häkkinen*, 2002; *Greene et al.*, 2012]. These studies suggest that changes in the volume of low-salinity water exported from high latitudes can alter the hydrographic conditions downstream through advection [*Petrie and Drinkwater*, 1993; *Smith et al.*, 2001] and may lead to the observed changes in the ecosystem structure and function [e.g., *Greene and Pershing*, 2007; *Ji et al.*, 2007, 2008; *Greene et al.*, 2012].

In a system that is dominated by advective processes, it is surprising that relatively little attention has been paid to the effect of local wind forcing in modulating freshwater transport on the Northwest Atlantic shelf. This is true, despite long-standing evidence of wind-induced along-shelf current variability [*Smith*, 1983, 1989; *Schwing*, 1992a, 1992b; *Loder et al.*, 1998a, 1998b] and subtidal sea level fluctuations that are coherent with the along-shelf wind stress at long spatial (O (10^3 km)) and temporal (synoptic to multiyear) scales

[*Noble and Butman*, 1979; *Sandstrom*, 1980; *Thompson*, 1986; *Schwing*, 1989; *Greenberg et al.*, 1997]. A lack of continuous long-term measurements makes it difficult to quantify the local wind effects on interannual time scales. However, by analyzing data over the period 1967–1970, *Sandstrom* [1980] demonstrated that multiyear sea level changes are coherent with alongshore winds over a wide band of frequencies, with increasing coherence at longer periods. Similarly, *Smith* [1989] showed that year-to-year flow anomalies in the coastal currents off southwest Nova Scotia were predominantly wind-driven at all depths in a 6.5 year time series of current measurements.

The purpose of this study is to investigate the influence of interannual variations in alongshore winds on the hydrodynamic and hydrographic properties within the NSS-GoM region (Figure 1). Specifically, we focus on understanding the modulation of sea level slope, along-shelf currents, and surface salinity by alongshore winds. In section 2, we describe the long-term observational data sets derived from multiple sources and conduct scaling analysis using a simplified momentum balance model that accounts for the dominant features. In section 3, we diagnose the response of along-shelf and cross-shelf sea level slope, along-shelf velocity, and surface salinity to alongshore wind forcing using coherence and correlation analyses. The relation between alongshore winds and large-scale forcing indices are examined using serial correlation analysis. In section 4, we propose a mechanism to explain the role of wind in modulating the flows on the Northwest Atlantic shelf and discuss its implications for the assessment of regional salinity variability and ecosystem changes.

2. Data and Methods

2.1. Data Sets

Wind observations were acquired for the period 1957–2011 at stations Sydney and Sable Island, Canada (270 km apart, see Figure 1 for locations). The data are provided by Environment Canada and made available via the Atlantic Zone Monitoring Program (AZMP) website. The wind record was decomposed into along-shelf $(+\tau_y = 250^\circ\mathrm{T})$ and cross-shelf $(+\tau_x = 340^\circ\mathrm{T})$ components based on the NSS orientation, where °T represents angle from true north. Wind stress was estimated from wind speed and direction at 1 h intervals using the quadratic stress law with a variable drag coefficient C_d [*Smith*, 1980, equation (14)] and then averaged to produce monthly and weekly mean values in order to compare with along-shelf sea level differences and cross-shore sea level slope. Finally, a 450 day running mean was applied to remove the seasonal and higher frequency signals. In order to evaluate the performance of this filter, we compared it with two other filters most commonly used in oceanography (fast Fourier transform (FFT)-based filter pl66tn and annual anomalies of deseasoned data). The three methods gave comparable results. However, the 450 day running mean was chosen, because it could handle short time series at no loss of temporal resolution (see Appendix A for detailed discussion).

Monthly averaged sea level records were obtained for the period 1957–2011 from the Permanent Service for Mean Sea Level (PSMSL) [*Woodworth and Player*, 2003]. For the purpose of this study, only those tide gauge records spanning more than 45 years, with less than 10% missing data, were chosen. Further, stations located near major rivers or in the inner GSL were excluded. With these restrictions, four tide gauge stations were selected: St John's, Halifax, Yarmouth, and Boston (Figure 1). The elevation records were corrected for the inverse barometer effect following *Ponte* [2006] using monthly sea level pressure obtained from the 2.5 × 2.5° National Center for Environmental Prediction (NCEP) reanalysis product (http://www.esrl.noaa.gov/psd/data/gridded/data.ncep.reanalysis.derived.surface.html) [*Kalnay et al.*, 1996]. In order to explore the shelf-wide adjustment of sea level slope in response to alongshore wind, the along-shelf sea level difference ($\Delta\eta_y$) was calculated as the difference between the northernmost station, St John's, and the other three stations. Since this study is focused on the interannual time scale, a 450 day running mean was applied to remove the seasonal and higher-frequency signals.

In order to estimate changes in cross-shelf sea level slope without information from offshore tide gauges, gridded Sea Surface Height Anomaly (SSHA) data were obtained from the NASA TOPEX/Poseidon (T/P) mission. The data set provides weekly mean SSHA on a 1/3° grid, spanning a period of 16 years from 1993 to 2008. The T/P satellite obtains high-accuracy altimetry data every 10 days along its ascending and descending ground tracks (~5.8 km), with the descending ground tracks approximately in alignment with the cross-shelf direction and perpendicular to the dominant shelf-scale flows. Although there have been concerns

about the limitations of altimetry data in near-shore regions (i.e., distinct tidal aliasing, uncertainties in the geoid), the T/P product has been corrected for various instrumental and environmental effects [*Benada*, 1997], and the general consistency among T/P satellite altimetry, tide-gauge data, and numerical hydrodynamic models over the NSS have been demonstrated by *Han* [2002] and *Han et al*. [2002]. The analyses performed in this study are for the same region, with three cross sections (S1–S3) at the western, central, and eastern sides of the NSS (Figure 1). Each section encompasses 4–5 nodes of the T/P grid. At each section, SSHA was corrected for the inverse barometer effect using the same method as for tide gauge stations, and the cross-shelf sea level slope ($\partial\eta/\partial x$) was calculated as the SSHA difference between the most offshore and inshore nodes divided by the distance between the two nodes. For each section, a 450 day running mean was applied to the weekly time series of $\partial\eta/\partial x$ to filter out the seasonal and higher-frequency signals.

Multiyear current measurements are available for the period October 1993 to September 1996 from mooring C2, deployed as part of the earlier GLOBEC mooring program [*Smith et al*., 2001]. The mooring was deployed on the 110 m isobath (43.04°N, 65.78°W, Figure 1), with two current meters that provided measurements at middepth (48 m) and near the bottom (98 m). The inflow from the inshore branch of the SSC into the GoM was captured by the along-isobath $(+v{=}260°\mathrm{T})$ component at the C2 site. To assess the interannual variability, the hourly records were detided with a 34 h low-pass filter (pl66tn) [*Beardsley and Rosenfeld*, 1983] and subsequently averaged using a 450 day running mean to remove the seasonal cycle.

Long-term records of salinity from 1978 to 2008 were obtained from the Department of Fisheries and Oceans (DFO) Canada climate database maintained at Bedford Institute of Oceanography. The database includes all available U.S. and Canadian survey data, reporting salinity at standard depths (10 m intervals from 0 to 150 m, and 20 m intervals from 170 to 290 m). In order to reduce biases introduced by gaps in the spatial and temporal distribution of observations, the database reports regional averages within 126 separate subregions on the Northwest Atlantic shelf. The subregions are distinguished based on topography and dominant oceanographic features (e.g., shallow areas, deep basins, bays, and major currents). Water-column properties are averaged within each subregion by month for each year, regardless of the number of stations per month [*Petrie et al*., 1996a, 1996b]. In this study, 17 subregions were excluded from the present analysis because they lack a sufficient number of salinity records (<60 records) and/or are located off-shelf (water depths greater than 1500 m). For each selected subregion, a time series of surface salinity was constructed by averaging the observed salinity between 0 and 30 m; however, the resulting time series is not available in all months of each year. In order to focus on the interannual variability, the time series was further averaged over the 31 year period 1978–2008 to obtain a long-term monthly climatology, and then the climatology was subtracted to remove seasonal variation, producing a time series of sea surface salinity anomalies (SSSA), which, for simplicity, will be termed "deseasoned" [cf., *Drinkwater and Gilbert*, 2004].

In order to determine if the wind variability is associated with large-scale atmospheric or oceanic forcing, the monthly North Atlantic Oscillation (NAO) index and the Gulf Stream North Wall (GSNW) index were examined. The monthly NAO index dating back to 1950 was obtained (see http://www.cpc.ncep.noaa.gov/data/teledoc/nao.shtml). It is derived using the leading empirical orthogonal function of sea level pressure anomalies over the Atlantic sector 20°N–80°N, 90°W–40°E, tracking the seasonal movements of the Icelandic low and Azores high throughout the year. In comparison to station-based winter indices, it provides less noisy and more optimal representation of the full spatial patterns of the NAO over the North Atlantic Ocean [*Hurrell et al*., 2013]. The GSNW index is defined as the northward extent of the Gulf Stream after it separates from the coast, and it is a measure of changes in the large-scale ocean currents. The monthly GSNW spanning the period 1966–2012 was obtained from http://www.pml-gulfstream.org.uk/default.htm [*Taylor and Stephens*, 1980]. The index is derived from a principal component analysis of the latitudinal position of the Gulf Stream's north wall measured at six longitudes between 79°W and 65°W, effectively capturing coherent variations in Gulf Stream position downstream of its separation from the coast.

2.2. Scaling Analysis Using a Simplified Momentum Balance Model

Scaling analysis using a simplified momentum balance model is conducted to quantify the responses of both sea level slope and along-shelf flow to the alongshore wind forcing. A right-hand Cartesian coordinated system is used here, with the *y* axis parallel to the coastline and positive toward the northeast and the *x* axis perpendicular to the *y* axis and positive offshore. Given the temporal and spatial dimensions of

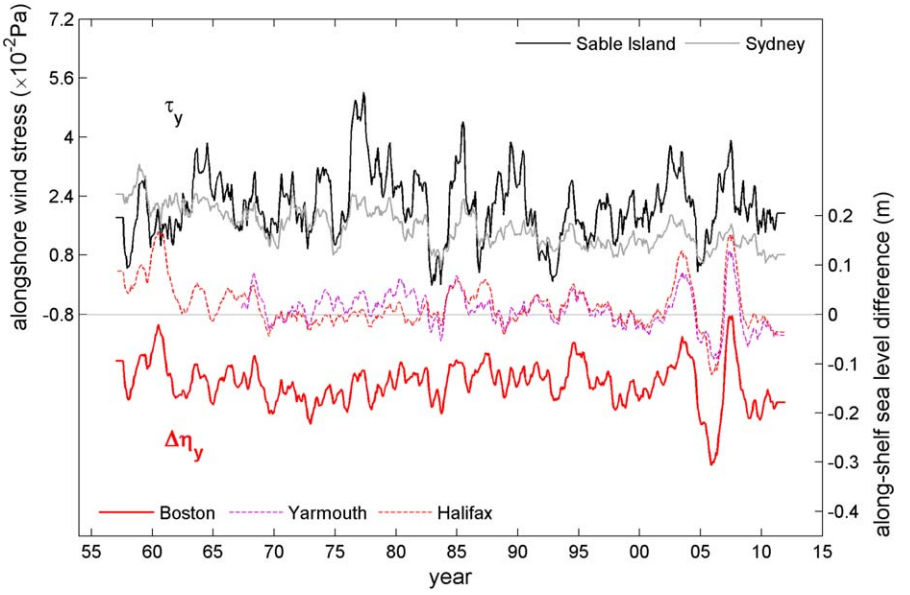

Figure 2. Time series of along-shelf wind stress (τ_y) and sea level differences ($\Delta\eta_y$) for the period 1957–2011. The gray scale lines show alongshore wind stress (250°T) at Sable Island (black) and Sydney (gray). The colored lines represent the along-shelf sea level differences between St John's and three southern stations: Boston, Yarmouth, and Halifax. A 450 day running mean is applied to the time series to remove the seasonal and higher frequency signals.

interest, several assumptions can be made: (1) the system is strongly affected by the earth's rotation $(Ro \ll 1)$, (2) the time scale is interannual $(\omega \ll f, \quad 1/\partial t \approx 0)$, and (3) the dynamic balance in the cross-shelf direction is geostrophic to first order [*Noble et al.*, 1983]. Applying these assumptions yields a quasi-steady model, with the principle terms in the momentum balance being [cf. *Csanady*, 1982],

$$g\frac{\partial \eta}{\partial y} = -\frac{g}{\rho}\int \frac{\partial \rho}{\partial y}dz - fu + \frac{\tau_y}{\rho h_s} - \frac{\tau_{by}}{\rho h_b} \tag{1}$$

$$g\frac{\partial \eta}{\partial x} = -\frac{g}{\rho}\int \frac{\partial \rho}{\partial x}dz + fv \tag{2}$$

where g is the gravitational acceleration (m s^{-2}), η is the sea surface height (m), ρ is the density of sea water (kg m^{-3}), τ_y is the alongshore wind stress (Pa), τ_{by} is the alongshore bottom stress (Pa), h_s and h_b are the surface and bottom layer thickness (m), f is the Coriolis parameter (s^{-1}), and u,v are the cross-shelf and along-shelf velocity, respectively (m s^{-1}). Equation (1) demonstrates that changes in along-shelf sea level slope (term on the left-hand side) are balanced by variations in along-shelf baroclinicity, the Coriolis acceleration acting on cross-shelf velocity, the alongshore wind forcing, and the along-shelf bottom friction (the four terms on the right-hand side), respectively. Earlier studies have shown that variations in sea surface elevation over a seasonal cycle are dominated by the baroclinic component, driven by GSL outflow, and modified by the wind-driven and remotely forced components [*Loder et al.*, 1997; *Han et al.*, 2002]. However, on interannual time scales, our results suggest that the flow is significantly modulated by alongshore wind stress (more details in section 3.3).

3. Results

3.1. Response of Along-Shelf Sea Level Slopes to Alongshore Wind

Interannual variations are observed in time series of both alongshore wind stress τ_y and sea level differences $\Delta\eta_y$ (Figure 2). On average, τ_y is positive (southwesterly or northeastward), measuring 1.56×10^{-2} and 2.14×10^{-2} Pa at Sydney and Sable Island, respectively (Table 1). Considerable deviations are observed at both sites, reaching 40–53% of the mean values (Table 1). τ_y is stronger at the offshore station (Sable Island),

Table 1. Observational Mean and Standard Deviation of Monthly Time Series of Alongshore Wind Stress τ_y and Along-Shelf Sea Level Difference $\Delta\eta_y$[a]

Stations	Period	Number of Data	Mean ± Standard Deviation
Alongshore Wind Stress[b] ($\times 10^{-2}$ Pa)			
Sydney	1957–2011	660	1.56 ± 0.61
Sable Island	1957–2011	660	2.14 ± 1.14
Along-Shelf Sea Level Difference From Station St John's (m)			
Halifax	1957–2011	660	0.02 ± 0.06
Yarmouth	1967–2011	544	0.01 ± 0.05
Boston	1957–2011	660	−0.14 ± 0.06

[a]A 450 day running mean is applied to remove seasonal and higher frequency fluctuations.
[b]The monthly wind stress is averaged from hourly data.

which is more representative of conditions over open water as suggested by previous studies [*Petrie and Smith*, 1977; *Sandstrom*, 1980; *Manning and Strout*, 2001]. Apart from the magnitude, temporal variations are similar between the two stations (Table 2, r = 0.51, $p < 0.01$). For example, the two stations experience low (i.e., 1957, 1984, 1993, and 2006) and high winds (i.e., 1959, 1977, 1987, 2003, and 2008) at approximately the same time. A similar pattern is also revealed in long-term NCEP wind products over the region (not shown). The correlation is high for sea level differences $\Delta\eta_y$ calculated at Halifax, Yarmouth, and Boston, downstream from St John's (Table 2, r > 0.68, $p < 0.01$) with zero-phase lag. Given the separation distance (200–400 km) between these stations, this suggests that the sea level slope responds over large spatial scales.

Over the period 1957–2011, $\Delta\eta_y$ and τ_y were positively correlated, so that a low (high) value $\Delta\eta_y$ coincides with weak (strong) wind (Table 2). For example, the alongshore wind stress was weak in 1984, 1993, and 2006, while $\Delta\eta_y$ in these years showed negative anomalies relative to the long-term mean. Similarly, positive anomalies of $\Delta\eta_y$ correspond to strong winds in 1977, 1985, 2002–2003, and 2008. Interestingly, the magnitude of the sea level response to changes in alongshore wind stress is not always equal for winds of the same magnitude. In general, interannual variations in $\Delta\eta_y$ tend to be stronger after 2000. For instance, the alongshore wind stress was weak and of comparable magnitude in 1984, 1993, and 2006. However, while $\Delta\eta_y$ increased by approximately equal amounts in 1984 and 1993, it was roughly doubled in 2006. This observation suggests that other drivers (i.e., freshening-induced baroclinicity) may work in opposition to (concert with) the alongshore wind stress to reduce (amplify) the sea level response. For instance, using the DFO hydrographic data set (see section 2 for details), we estimated the baroclinic pressure gradient (first

Table 2. Correlations Between Low-Pass Filtered Alongshore Wind Stress (τ_y), Along-Shelf Sea Level Differences ($\Delta\eta_y$), and Cross-Shelf Sea Level Slope ($\partial\eta/\partial x$)[a]

Stations[b]		Correlation Coefficient (*r*)	Time Period	Number of Records (*n*)
τ_y (monthly)[c]				
Sydney	Sable Island	0.51	Jan 1957–Dec 2011	660
$\Delta\eta_y$ (monthly)				
Halifax	Boston	0.85	Jan 1957–Dec 2011	660
Yarmouth	Halifax	0.68	Sep 1966–Dec 2011	544
Boston	Yarmouth	0.74	Sep 1966–Dec 2011	544
τ_y and $\Delta\eta_y$ (monthly)[c]				
Sydney	Halifax	0.44	Jan 1957–Dec2011	660
Sydney	Yarmouth	0.58	Sep 1966–Dec 2011	544
Sydney	Boston	0.36	Jan 1957–Dec 2011	660
Sable Island	Halifax	0.11	Jan 1957–Dec 2011	660
Sable Island	Yarmouth	0.44	Sep 1966–Dec 2011	544
Sable Island	Boston	0.29	Jan 1957–Dec 2011	660
τ_y and $\partial\eta/\partial x$ (weekly)[d]				
Sydney	S3	0.46	Jan 1993–May 2009	854
Sydney	S2	0.64		
Sydney	S1	0.73		
Sable Island	S3	0.43		
Sable Island	S2	0.53		
Sable Island	S1	0.67		

[a]The raw data are obtained in hourly, monthly, and weekly format (see section 2 for details). A 450 day running mean filter was applied to eliminate seasonal and higher frequency signals. In order to correlate any observation pair of different resolutions, the finer resolution time series was averaged to the coarser resolution, and the resulting data interval, the time period, and the number of records (n) were given. All the correlation coefficients are significant at $p < 0.01$.
[b]Stations are listed from north to south along the shelf.
[c]Wind data were averaged from hourly to monthly.
[d]Wind data were averaged from hourly to weekly.

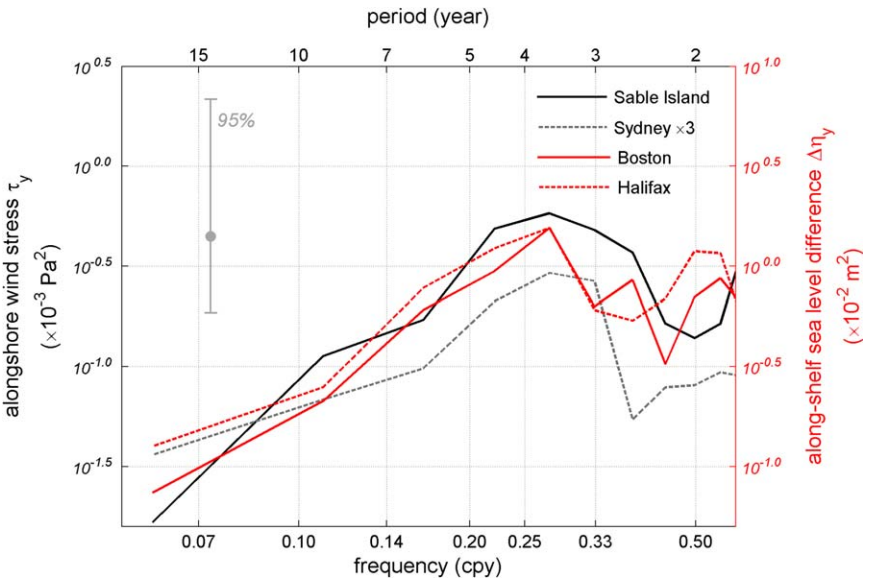

Figure 3. Power spectra (variance preserved) of low-passed time series for alongshore wind stress τ_y at Sable Island and Sydney as well as the along-shelf sea level differences $\Delta\eta_y$ between station St John's and two stations: Boston and Halifax. The abbreviation cpy stands for cycles per year. The horizontal axis is plotted in logarithmic scale. Representative 95% confidence intervals are shown.

term on the right-hand side of equation (1)) between the western and eastern end of the NSS. The long-term mean was -6.3×10^{-7} m s^{-2} over the period 1978–2008, on the same order as the wind forcing. During 1984 and 1993, the baroclinicity was -5.8×10^{-7} and -5.5×10^{-7} m s^{-2}, respectively. The positive anomalies associated with the baroclinic pressure gradient weaken the wind-induced negative anomalies of $\Delta\eta_y$. Conversely, the baroclinicity in 2006 was -7.7×10^{-7} m s^{-2}, a negative anomalies relative to the long-term mean, which reinforces the wind-induced negative anomalies of $\Delta\eta_y$.

The correlation between $\Delta\eta_y$ and τ_y suggests that the alongshore wind stress could be one factor driving changes in sea level slope. We now examine whether changes in τ_y can account for the observed changes in $\Delta\eta_y$. Low-passed spectra are constructed to identify the dominant energy bands in both records. For alongshore wind stress, both stations have similar peaks centered on 2.5–7 years (Figure 3), though the power is about three times more at Sable Island due to the increased wind speed offshore. Similarly, peaks are observed in identical frequency bands in the spectra of $\Delta\eta_y$ (Figure 3). Coherence between $\Delta\eta_y$ and τ_y is consistently high, above 0.5, and significant (at 95% confidence) for variations between 2 and 7 years (Figure 4a). There is a 40° phase lag between τ_y and $\Delta\eta_y$ across all energetic frequency bands (Figure 4b), which suggests a dynamic link whereby along-shelf sea level slope responds to alongshore wind stress via wind-induced motions. This lag represents an approximately 3–10 month response time for fluctuations having periods ranging from 2 to 7 years. The weak frequency dependence of the phase lags implies that the response of the along-shelf sea level slope is largely linear, in agreement with the analytical expression derived by *Schwing* [1992b].

The wind-induced gain (loss) of $\Delta\eta_y$ can be quantified using the third term on the right-hand side of equation (1),

$$\Delta\eta_y = \frac{\tau_y L}{g\rho h_s} \tag{3}$$

Choosing $L = 10^6$ m to represent the distance between the St Johns' and Halifax tide gauge stations, $\tau_y = 1.14 \times 10^{-2}$ Pa, as the variation in along-shelf wind stress at Sable Island, and $h_s = 25 - 50$ m for the vertical scale where surface stress vanishes, yields $\Delta\eta_y = 0.023 - 0.047$ m. This is a moderate portion (40–80%) of the observed variation in along-shelf sea level difference (0.06 m, Table 1). The results are similar when using other tide gauge stations. Thus, the interannual changes in alongshore wind stress account for a substantial portion of the observed interannual variations in $\Delta\eta_y$.

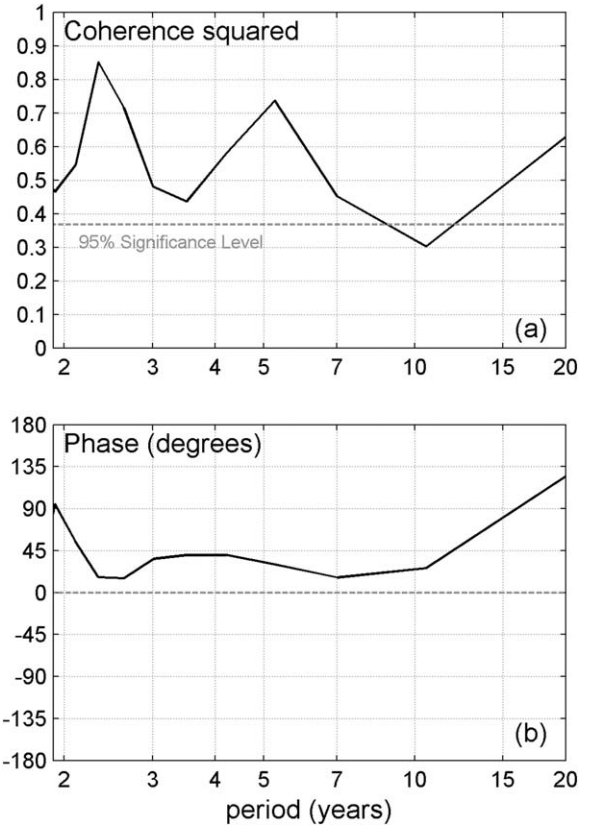

Figure 4. (a) Coherence squared and (b) phase between along-shelf sea level differences (St John's–Boston) and alongshore wind stress at Sable Island (250°T) for the period 1957–2011. Positive phase indicates wind leading sea level differences (degrees of freedom = 73; 95% significance level = 0.37, dashed line in Figure 4a).

3.2. Responses of Cross-Shelf Sea Level Slope to Alongshore Wind

In the along-shelf direction, the tide gauge data have shown that the alongshore winds modulate along-shelf sea level slope. The next step is to examine the along-shelf motion associated with this sea level adjustment. Unfortunately, long-term current measurements spanning more than 50 years are not available. Therefore, indirect evidence is needed. Given that the primary cross-shelf balance is geostrophic (equation (2)), it is reasonable to diagnose changes in the along-shelf flow based on the cross-shelf sea level slope.

The cross-shelf sea level slope ($\partial\eta/\partial x$) is derived from altimetric SSHA for the period 1993–2008. Even though the time period is relatively short, it is still representative since the wind stress exhibits strong interannual variability (0.003–0.039 Pa) over this 16 year time period (Figure 5). Positive correlations are found between $\partial\eta/\partial x$ and τ_y during this period. Specifically, positive $\partial\eta/\partial x$ anomalies coincide with strong τ_y (i.e., 2002–2003 and 2007) and vice versa. The correlation coefficients (r) are 0.67, 0.53, and 0.43 for sections S1–S3, respectively (Table 2, $p < 0.01$).

The correlation agrees well with the pattern depicted from the momentum balance model. On average, the cross-shelf sea level on the NSS is high inshore and low offshore, leading to a negative $\partial\eta/\partial x$ that is balanced by the Coriolis acceleration acting on the southwestward mean flow in a geostrophic sense. During periods of stronger alongshore (southwesterly or northeastward) winds, the mean flow is weakened, such that the cross-shelf sea level slope is flattened, yielding positive $\partial\eta/\partial x$ anomalies. In contrast, the relaxation of alongshore winds (weaker τ_y) allows stronger southwestward flow to develop, which sharpens cross-shelf sea level slope and leads to negative $\partial\eta/\partial x$ anomalies.

In addition, the temporal and spatial scales associated with the cross-shelf sea level response are consistent with those determined from the along-shelf sea level response (section 3.1). The variations are coherent over the entire shelf, suggesting that the horizontal adjustment scale is at least of O(100) km. Over the relatively short record, the dominant variations are visualized at a period of 3–5 years (Figure 5), similar to the dominant frequency bands observed in alongshore winds and along-shelf sea level differences (Figure 3).

3.3. Responses of Along-Shelf Flow to the Alongshore Wind

The satellite-derived altimetry data captures the wind-induced cross-shelf sea level adjustment reasonably well as shown in the last section. Hence, further analysis is warranted to estimate the associated change in along-shelf surface velocity associated with $\partial\eta/\partial x$ anomalies, especially for the inshore branch of the along-shelf flow. The focus here is on the along-shelf velocity at the sea surface where the baroclinic component

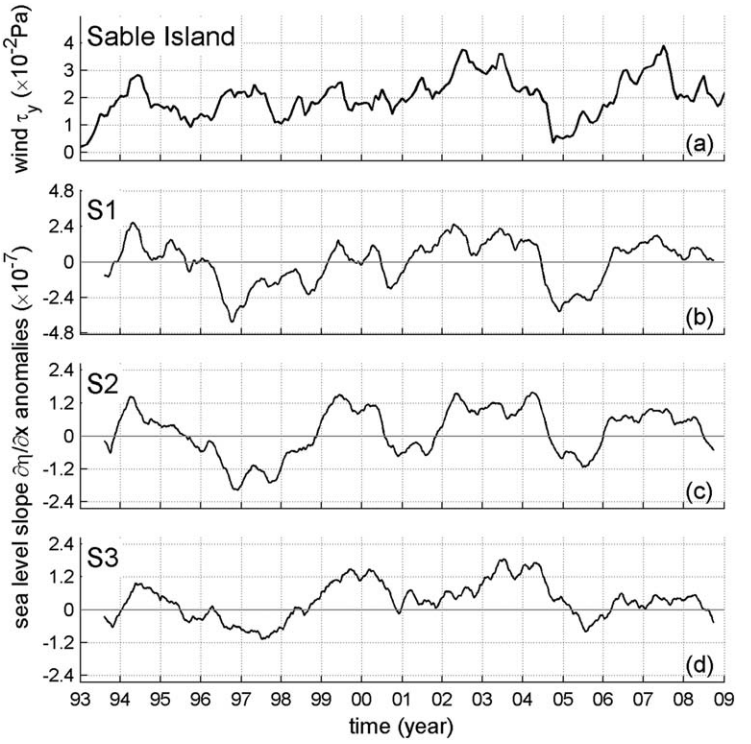

Figure 5. (a) Time series of the alongshore wind stress (250°T) and (b–d) the cross-shelf sea level slope along the sections S1, S2, and S3 on the Nova Scotian Shelf (see Figure 1 for the locations). The sea level slope is calculated from weekly altimetry data between 1993 and 2008. A 450 day running mean is applied to all the time series.

is minimized, allowing us to neglect the baroclinic pressure gradient in equation (2). The along-shelf flow (v) then can be computed as

$$v = \frac{g}{f}\frac{\partial \eta}{\partial x} \tag{4}$$

The results show temporal patterns that are quantitatively similar at the three cross sections, from S1 in the west to S3 in the east. Here we will focus on the results from S1, as it is located nearest to the current meter mooring C2.

The along-shelf velocity anomalies at the western section vary from about -4×10^{-2} to 2×10^{-2} m s^{-1} (Figure 6), which are significant in comparison to previous reported mean velocities of 7×10^{-2} to 12×10^{-2} m s^{-1} [*Hannah et al.*, 2001] and seasonal variations of 6×10^{-2} to 10×10^{-2} m s^{-1} [*Hannah et al.*, 2001; *Han et al.*, 2002] in the NSS region. The velocity anomalies and alongshore wind stress are significantly correlated with the following general pattern: stronger winds correspond with positive (northeastward) current anomalies, opposite the mean flow on the shelf, whereas weaker winds favor negative (southwestward) current anomalies that are in the same direction as the mean flow. Although there is an exception around 1996–1997, the alongshore wind stress is likely a significant driver of along-shelf current variability, potentially responsible for 20–47% of the total variations over the 16 year period. The mismatch in 1996–1997 may reflect other forcing mechanism, including cross-shore winds (with maximum of 2.7×10^{-2} Pa yielding $\sim 1 \times 10^{-2}$ m s^{-1} along-shelf velocity based on Ekman balance), the passage of remote waves through the study region, or the increased freshwater discharge that led to strong baroclinic forcing (negative salinity anomalies on the shelf from 1996 to 1997, see Figure 8, cf. *Drinkwater and Gilbert* [2004]).

In addition to the velocity anomalies inferred from the altimetry data, GLOBEC mooring C2 (Figure 1) reported current measurements from 1993 to 1996, capturing the inshore branch of the SSC that flows along the coast into the GoM [*Smith et al.*, 2001]. Although the length of the time series is rather short, the comparison is still worthwhile because the data capture two consecutive years with contrasting wind

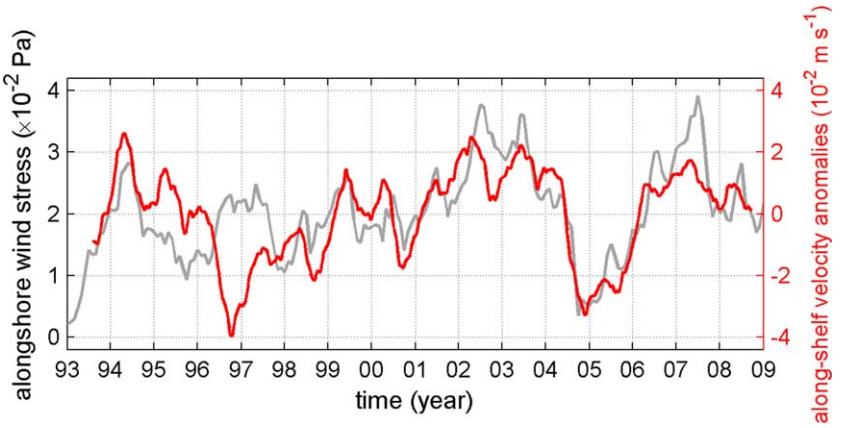

Figure 6. Time series of alongshore wind stress at Sable Island and along-shelf velocity anomalies inferred from SSHA at section S1 (see Figure 1 for location). A 450 day running mean is applied to both time series to remove the seasonal and higher frequency fluctuations. For the along-shelf velocity anomalies, negative values represent southwestward flow (the same direction as the mean flow).

regimes (Figure 7). Observations show increased flow into the GoM associated with relaxing winds between 1994 and 1995. The inflow increases as the alongshore wind stress switches from relatively strong to weak conditions (with respect to the long-term mean, 2.14×10^{-2} Pa), followed by a gradual rebound in 1996. Despite the fact that these observations were made away from the surface, at mid-depth (48 m) and near the bottom (98 m), the oscillation of the inflow still covaries with the alongshore wind. The current magnitude ranges from 2×10^{-2} to 3×10^{-2} m s^{-1}, amounting to roughly 20% of the long-term mean at this site [*Smith*, 1983, 1989]. This suggests that interannual changes in the strength of the SSC appear to be governed, to some extent, by wind-induced modulation in the NSS-GoM region.

3.4. Responses of Surface Salinity to Alongshore Wind

In an advectively dominated system such as this one, the dynamic response of along-shelf currents described above suggests that alongshore winds may also modulate the transport of less saline waters along the shelf. To examine if alongshore winds play a role in controlling the SSSA, long-term observations (1978–2008) are analyzed in four regions, including the Newfoundland Shelf (NF), GSL, NSS, and GoM.

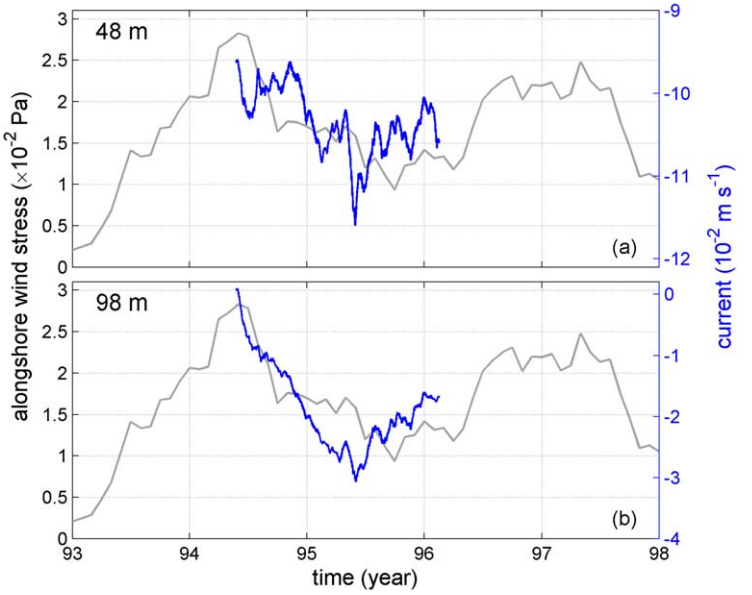

Figure 7. Time series of alongshore wind at Sable Island and currents in the mid and lower water column at GLOBEC buoy C2 (see Figure 1 for location). A 450 day running mean is applied to both time series to remove the seasonal and higher frequency fluctuations. For the current, the direction is defined as 260°T along-isobath, so that negative values represent inflow into the GoM.

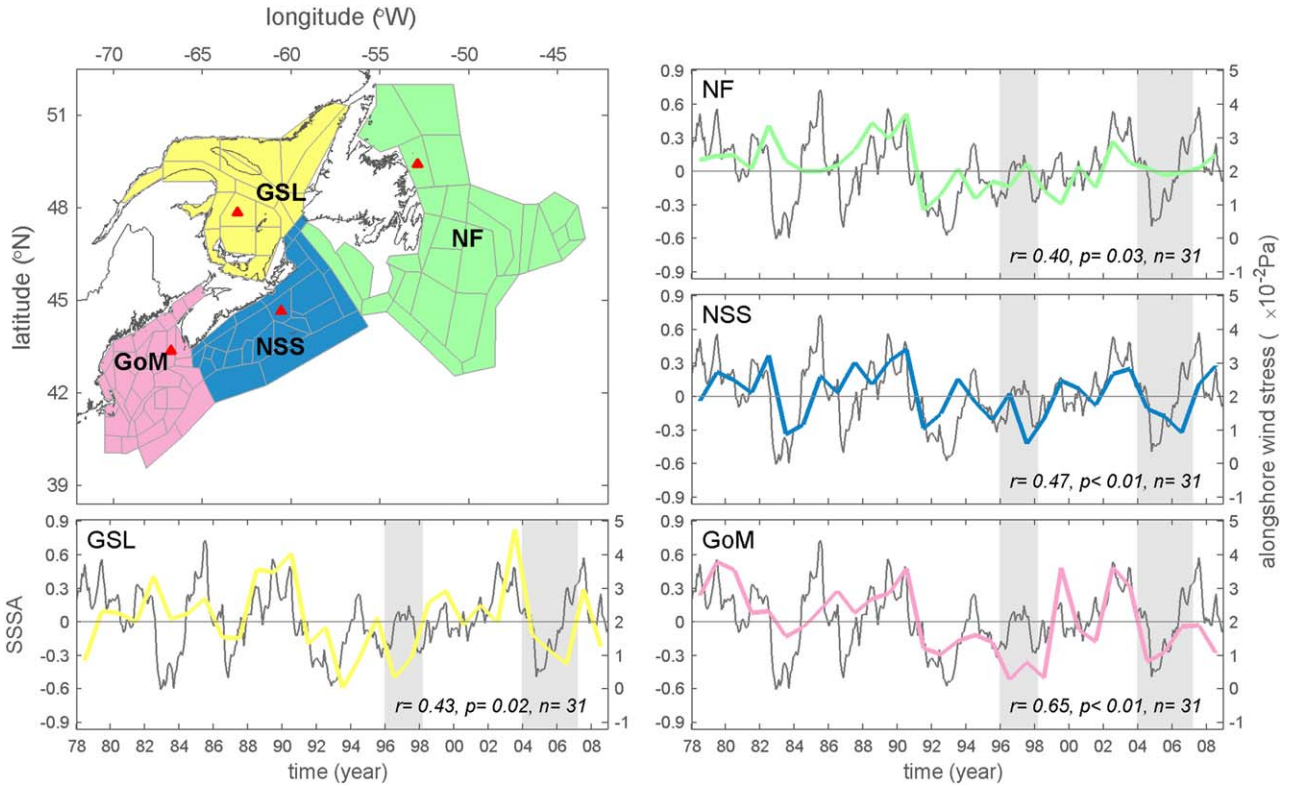

Figure 8. Survey polygons in the Northwest Atlantic region where salinity data are collected, including the Newfoundland Shelf (NF), Gulf of St. Lawrence (GSL), Nova Scotian Shelf (NSS), and Gulf of Maine (GoM). The red triangles denote four polygons that represent their respective subregions. Time series show the alongshore wind stress at Sable Island (gray line) and annual sea surface salinity anomalies (SSSA, colored lines) in four subregions. Two recent freshening events in the GoM are shaded.

Figure 8 shows the survey polygons as well as a time series of SSSA from four subregions representing the patterns of surface salinity within each polygon. The observed temporal pattern of SSSA reveals more negative anomalies (low-salinity or freshening) during the periods of 1982–1984, 1993–1998, and 2004–2006, and more positive anomalies (high salinity or saltification) during the periods of 1978–1982, 1988–1991, and 2002–2003, with the timing and peak of the anomalies slightly different from region to region. The variations are positively correlated with the alongshore wind stress ($r = 0.40–0.65$, $p < 0.05$), where positive

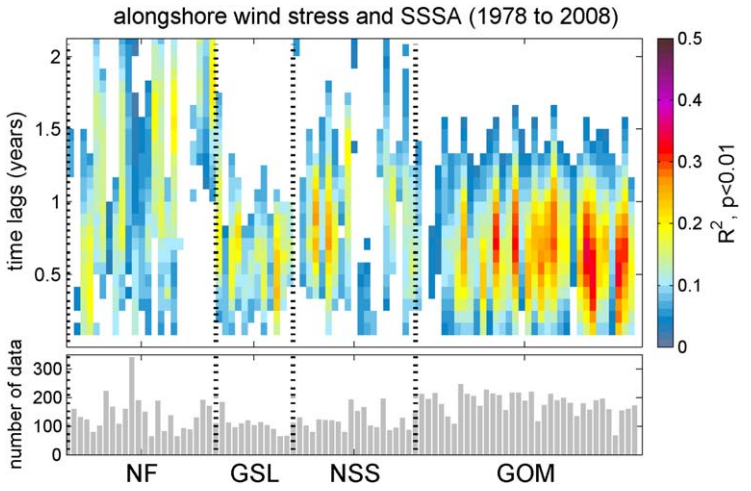

Figure 9. The lagged correlation (R^2) between alongshore wind and sea surface salinity anomalies in the Northwest Atlantic region, including the Newfoundland Shelf (NF), Gulf of St. Lawrence (GSL), Nova Scotian Shelf (NSS), and Gulf of Maine (GoM). A 450 day running mean is applied for the time series to remove the seasonal and subseasonal fluctuations.

SSSAs occur under the forcing of strong alongshore winds (above the long-term mean) and vice versa. This relationship supports the idea that weak (strong) alongshore winds favor (hamper) the southwestward advection of freshwater on the shelf, complemented by reduced (enhanced) vertical mixing, such that the observed SSSA displays fresher (saltier) patterns.

The relationship between the observed SSSA and alongshore winds are quantitatively examined for all survey polygons falling within the four regions. Here the time series of SSSA within each survey polygon is correlated at various lags to the alongshore wind stress taken from Sable Island. Although the SSSA data are discrete in time, the relationship still can be examined by selecting wind observations in the same month that the SSSA records were collected or for a number of months prior to the SSSA observations, if time lags are considered. In Figure 9, the results are only shown for significant values ($p < 0.01$). The varying magnitude of alongshore winds accounts for >20% of the variability in NF and GSL and >30% of the variability in the NSS-GoM region. The largest R^2 is found at time lags of 0.5–0.8 year (roughly 6–9.5 months) in the NSS-GoM region, which is in agreement with advection-induced time lags for this region [*Smith*, 1989]. Interestingly, this is also in agreement with the 3–10 month lags associated with the response of alongshore sea level slopes gradients to wind forcing (section 3.1).

3.5. The Relationship Between Alongshore Wind and Large-Scale Forcing

Even though the alongshore winds are important in modulating the hydrodynamic conditions on the Northwest Atlantic shelf, it is not clear thus far what influences the interannual variability of the winds. The NAO is a commonly used basin-scale index of atmospheric variability, that is, among other things, a much generalized predictor of large-scale wind patterns and their relative strength. By definition, positive phases of NAO provide that westerlies strengthen and shift north and vice versa [*Hurrell et al*., 2003]. The GSNW is an oceanographic index that is in part associated with the wind pattern (e.g., wind stress curl) in the North Atlantic [*Joyce et al*., 2000]. Several lines of evidence based on data prior to 2000 suggested that the GSNW follows the NAO with a lag of two years [*Taylor and Stephens*, 1998; *Hameed and Piontkovski*, 2004] or shorter [*Joyce et al*., 2000].

Based on visual inspection, alongshore winds and the two indices appear to exhibit synchrony over the period 1975–1990 (Figures 10a–10c), when the NAO and GSNW indices swing from negative to positive phase, there is concurrent weakening of the alongshore winds. But comparing the long-term NAO index with alongshore wind stress over the whole period 1960–2010 does not reveal strong correlations ($r = -0.02$, $p < 0.01$), neither does the GSNW index ($r = -0.10$, $p = 0.6$). The weak correlations may be due to the change in importance of the indices over time (also known as nonstationarity).

In order to examine the nonstationary linkages, serial correlation analysis is conducted with a 10 year moving window. A similar analysis was used by *Joyce* [2002] and *Hare and Kane* [2012] to show the correlation of environmental variables that has changed over time. The approach was performed between NAO and GSNW at a lag of 2 years (Figure 10d). They are significantly correlated early in the time series from 1970 to 2000, $r = 0.3$–0.8), which is consistent with aforementioned evidence [*Taylor and Stephens*, 1998; *Joyce et al*., 2000; *Hameed and Piontkovski*, 2004]. A recent breakdown between the two indices (below 95% significance level) is found after 2000. The relationship between alongshore winds and the two indices is examined using the serial correlation analysis. A significant negative correlation is found between the GSNW (with 2 year lag) and alongshore wind stress, with significance increasing after 1975 and peaking ($r = -0.6$) for the periods 1980–1985 and 2003–2005 (Figure 10e). The correlation between alongshore winds and NAO is significant and negative from 1965 to 1985 but breaks down later in the record. This finding suggests that shifts in basin-scale atmospheric patterns (indexed by the NAO) are likely responsible for adding variance to regional alongshore winds in early, but not recent, decades. A similarly high correlation over a limited period, along with a recent breakdown, was also reported in an analysis of the correlation between NAO and *Calanus finmarchicus* abundance over the last 20 years [*Hare and Kane*, 2012]. The decoupling between alongshore wind stress and NAO may represent an increased importance of local forcing after 1990, and these changes generally occur in conjunction with a recent breakdown of NAO-GSNW linkage and an elevated wind-GSNW correlation. The cause of the switch is not known and awaiting future investigation.

4. Discussion

The analyses of long-term observations in this study explicitly demonstrate significant wind modulation of sea level slope and along-shelf velocity on the Northwest Atlantic shelf. While previous work focused on

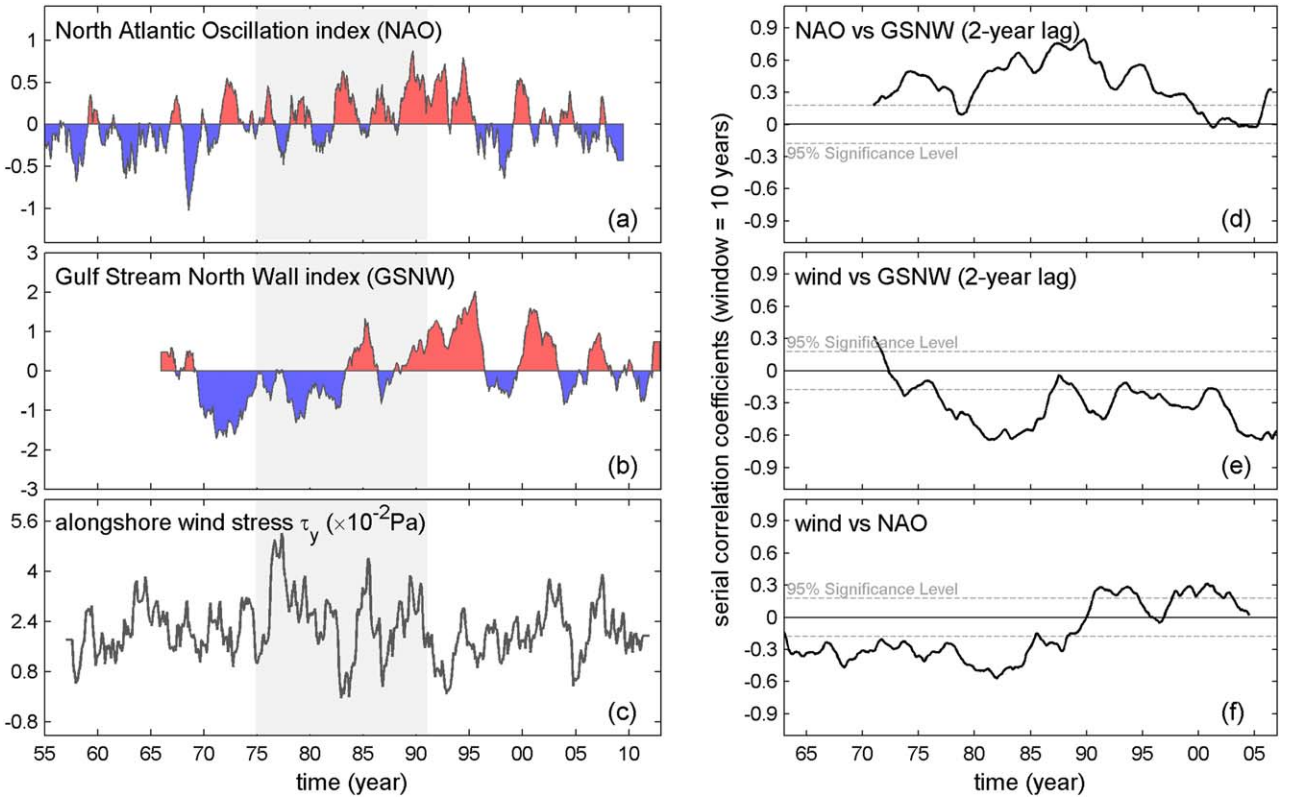

Figure 10. The time series of monthly (a) North Atlantic Oscillation index (NAO), (b) Gulf Stream North Wall index (GSNW), and (c) alongshore wind stress (250°T) at Sable Island. A 450 day running mean is applied to remove the seasonal and higher frequency fluctuations. (d–f) Serial correlations between NAO, GSNW, and alongshore wind stress. Correlations with GSNW are performed at a lag of 2 years for GSNW. Significance of correlations is denoted by gray dashed lines (degree of freedom = 118; 95% significance level = 0.18).

synoptic or seasonal time scales [*Noble and Butman*, 1979; *Sandstrom*, 1980; *Schwing*, 1989, 1992a, 1992b], the results from this study reveal the wind-induced adjustment on interannual time scales (2.5–7 years). The wind's role is similar to that in the synoptic and seasonal frequency bands in three ways. First, alongshore winds are an important source of energy, especially at periods of 2.5–7 years (Figure 3a). Second, there are significant wind-induced barotropic responses of sea level slope and velocity in the along-shelf direction. Third, to first order the cross-shelf balance is geostrophic (Figure 6). However, noticeable differences emerge in the phase lag between wind forcing and the adjustment: at periods less than 2 years, the phase lag is characterized by a strong dependence on wind frequency; but this dependence diminishes at interannual time scale of 2–10 years. In other words, the time lag becomes an approximately linear function of wind period (e.g., Figure 4b). The response agrees with the analytical expression derived by *Schwing* [1992b].

Many studies have examined the influence of wind forcing on coastal sea level fluctuations on the NSS, yet a dynamic link between alongshore winds, sea level slope, and along-shelf velocity has not been fully examined. The long-term wind modulation described in section 3 can be considered a frictional response of along-shelf velocity associated with the adjustment of sea level slope on the shelf. This relationship is conceptually illustrated in Figure 11. The southwestward flow and the southwesterly (northeastward) wind are nearly 180° out of phase. During stronger southwesterly wind, the southwestward velocity is weakened, and the along-shelf sea level slope tilts up in the direction of the wind as the excess water piles up upstream. This is accompanied by a depression in sea level near the coast as the along-shelf geostrophically balanced flow weakens. Therefore, in this state, the sea level exhibits a "high" anomaly in the upstream NF region. Conversely, under weaker southwesterly winds, the along-shelf flow becomes stronger, and the resulting sea level is elevated downstream and shoreward, so the overall pattern displays a high sea level anomaly near the GoM.

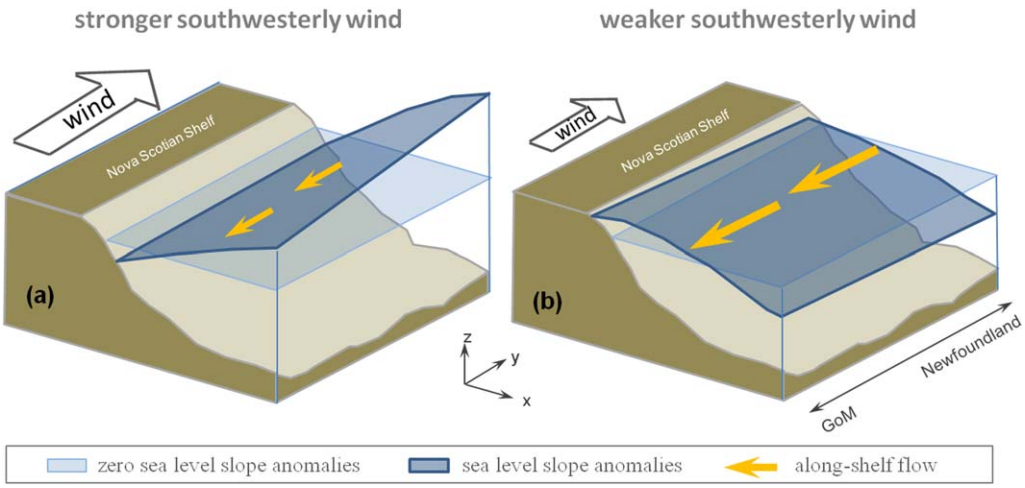

Figure 11. Schematic diagram for the modulation of sea level slope and flow by alongshore wind stress on the Northwest Atlantic shelf. (a) Under stronger southwesterly (northeastward) winds, the southwestward flow is weaker and induces upwind sea level slope along the shelf and a depression of sea level inshore via geostrophic relationship. Therefore, the overall sea level exhibits a high anomaly in the upstream Newfoundland Shelf (NF) region. (b) Under weaker southwesterly winds, the Scotian Shelf Current (SSC) becomes stronger, resulting in a sea level slope that tilts downstream and shoreward, so the overall pattern displays a high anomaly near the Gulf of Maine (GoM).

One of the key features in the aforementioned mechanism is the adjustment of the cross-shelf sea level slope, which behaves as a "valve" in "controlling" the strength of along-shelf flow. The valve tends to be more closed when the stronger alongshore winds induce depression of sea level inshore (Figure 11a), so the along-shelf velocity is largely reduced, regardless of the amount of the freshwater available from high-latitude sources. In contrast, the valve opens as the alongshore winds weaken (rise of cross-shelf sea level shoreward Figure 11b). This creates a favorable condition for strong shelf flow to develop, which in turn reinforces freshwater delivery from high-latitude sources into the Northwest Atlantic shelf region. The "valve" mechanism appears to influence the connection between the GoM and GSL. For instance, when the "valve" is "open," the timing of freshwater arrival at the GoM is likely to be shortened by the increased volume transport and the decreased advection time, and a more direct link would be expected between water properties in the two gulf systems.

The "valve" mechanism offers the possibility of assessing the alternations of salinity anomalies in the NSS-GoM region based on interannual changes in the alongshore wind stress. Recent studies have suggested that high-latitude freshening is a major forcing that influences interannual changes in hydrographic properties downstream. For example, the climate-forcing hypothesis proposes that changes in the amount of buoyancy released far upstream (i.e., Arctic Ocean) induce hydrographic variations seen on the Northwest Atlantic shelf [*Loder et al*., 2001]. However, our results offer yet another alternative that salinity anomalies could also be induced if the advection/propagation of source waters is modulated along its pathway by alongshore winds as illustrated by the "valve" mechanism. In the NSS-GoM region, the decadal-scale hydrographic changes are a common occurrence associated with several great salinity anomalies at high latitudes [*Loder et al*., 2001], yet large salinity anomalies were also observed with more than 0.5 on subdecadal or year-to-year time scales (Figure 8). On interannual time scale, the timing and magnitude of salinity variations are not solely explained by the remote sources of freshwater; rather, those are also complicated by the variable advection rate at which the buoyancy was transported from high latitude into the downstream region. From our analysis, the alongshore wind stress appears to be one of the potential drivers that can modulate the advection rate. An interesting follow-on study is to assess whether the alongshore wind stress should be considered a reliable predictor of the interannual variability of hydrographic conditions in the NSS-GoM region.

The complex response of the hydrographic conditions in the NSS-GoM region likely results from the competition between multiple mechanisms, and "valving" is one way to explain the interplay between mechanisms that may end up compounding or canceling one another out. Take the long-term SSSA for example. *Deese-Riordan* [2009] reported that the freshening between 2004 and 2005 in the GoM was associated with

an input of anomalously fresh and cold water from large St. Lawrence River discharge (indicated by RIVSUM) from the preceding winter, and the time lag suggested the advection of freshwater as the possible mechanism. However, the high discharge afterward in 2006 winter occurred without any associated freshening in the GoM. The apparent paradox (freshening versus salting) under similar discharge conditions implies the dominance of the "valve" mechanism, that is, weaker alongshore winds in 2004–2005 opened the "valve" for the buoyancy to be delivered into the GoM, while stronger alongshore winds in 2006 tended to close the "valve" and block the pathway (Figure 8). An example of mismatch was seen in 1996–1997 (Figures 6 and 8), when extremely low-salinity water propagating through the GSL and NSS region [*Drinkwater and Gilbert*, 2004] swamped the opposing wind mechanism. The increased freshwater discharge led to stronger cross-shelf baroclinic pressure gradients and, hence, an enhanced SSC.

Although our analyses demonstrate that interannual variations in along-shelf velocity may be caused by the frictional effect of alongshore wind stress, earlier studies have suggested that other forcing factors, such as the cross-shore wind stress [*Schwing*, 1992a, 1992b], baroclinic forcing [*Loder et al*., 2001], propagation of remote waves [*Schwing*, 1992a, 1992b], or bathymetric effects [*Greenberg et al*., 1997], may play a role in determining the temporal patterns. For instance, the mismatch between winds and currents in 1997 (Figure 6) may be a consequence of cross-shelf wind stress, a remote wave propagating into the study region, or freshening-induced baroclinic forcing. In this study, despite the oversimplification of details related to the lateral dynamics, the geostrophic relationship is instructive and serves as a reasonable first-order assumption. Using this assumption, we are able to explain 20–47% of the interannual variability in the along-shelf velocity between 1993 and 2008. While our results are encouraging, future comprehensive numerical modeling investigations are warranted to quantify the interannual variability caused by the joint effects of alongshore wind stress, buoyancy, and remote waves.

5. Summary

The analyses of long-term winds, sea level elevation, altimetry, current, and salinity data reveal significant wind modulation in the NSS-GoM region. The results show that interannual changes in along-shelf wind stress can explain 10–30% of the observed interannual variations in sea level slope and along-shelf flow. Using a simplified momentum balance model, the underlying mechanism is identified: stronger southwesterly (northeastward) winds resist mean southwestward flow on the shelf, whereas weaker winds favor the development of stronger flow. The associated sea level slope has distinct patterns under contrasting wind conditions, with high sea level anomalies located in the GoM (NF) region under weaker (stronger) winds. The results suggest that interannual fluctuations in wind forcing should be considered in combination with high-latitude freshening to explain recent hydrographic changes on the Northwest Atlantic shelf.

Appendix A

The goal of this study was to determine the importance of regional wind forcing in modulating advective processes and hydrographic properties along the Northwest Atlantic shelf on interannual time scales. To do this, it was necessary to low-pass filter measurements from a variety of sources, spanning different time periods with different temporal resolutions. The appropriate low-pass filter should effectively remove all seasonal and higher frequency variability from our time series independent of their record length or resolution and largely preserve the low-frequency fluctuations. For this, we selected three filters commonly used in oceanography: (1) running mean filter [e.g., *Smith et al*., 2012]; an FFT-based filter pl66tn [*Beardsley and Rosenfeld*, 1983]; and annual anomalies of deseasoned data [*Petrie and Drinkwater*, 1993].

We now compare the performance of the three filters using data sets analyzed in our study. As an example, we selected time series of alongshore wind stress, along-shelf sea level differences, and cross-shelf sea level slopes, each exhibiting strong seasonal variations and moderate interannual changes (Figures A1a–A1c). As shown in the spectra (Figures A1d–A1f), a 450 day cutoff period is sufficiently wide to eliminate all the seasonal variability (this does not exclude the choice of other cutoff periods that may also work). Despite some

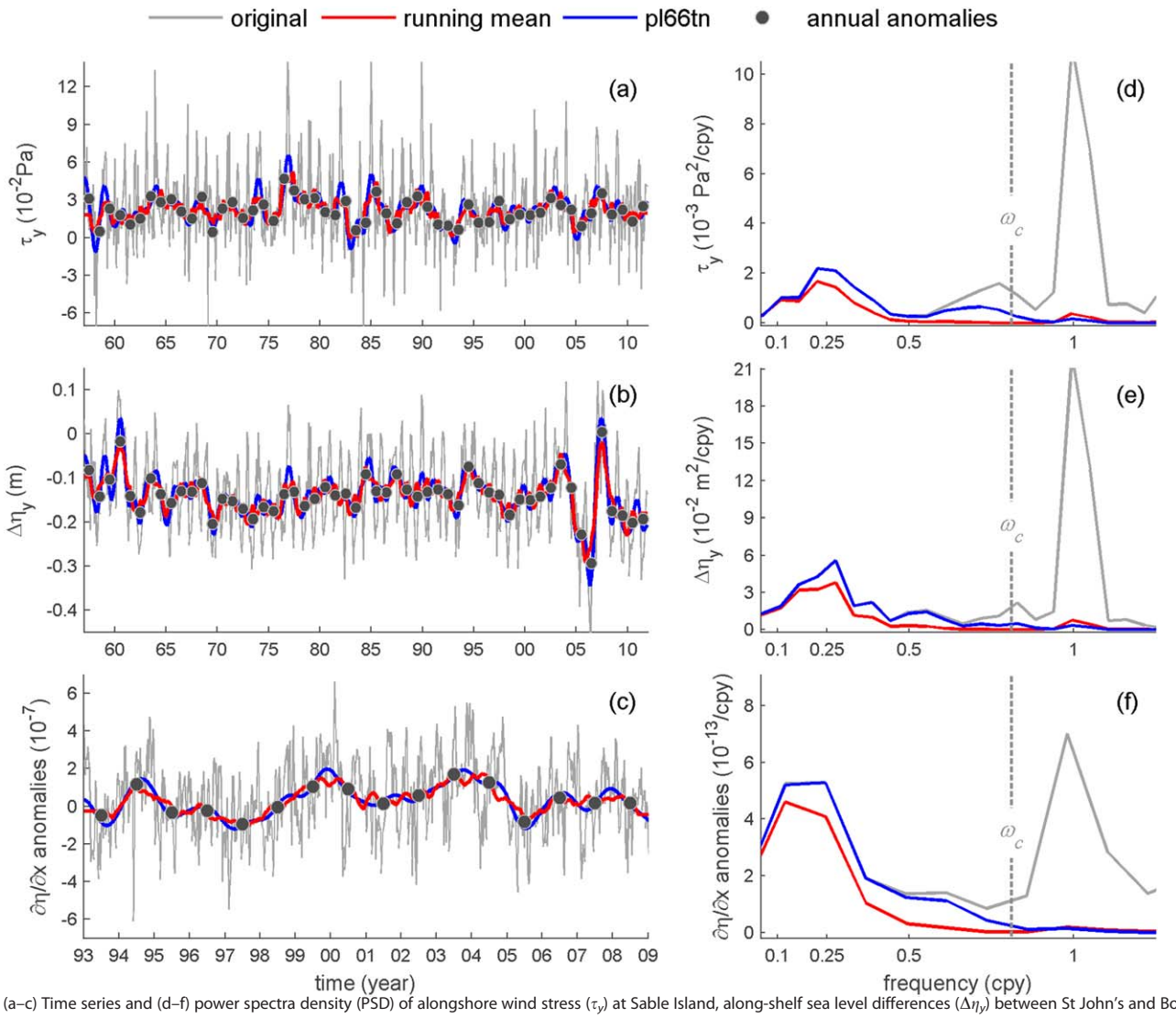

Figure A1. (a–c) Time series and (d–f) power spectra density (PSD) of alongshore wind stress (τ_y) at Sable Island, along-shelf sea level differences ($\Delta\eta_y$) between St John's and Boston, and cross-shelf sea level slope ($\partial\eta/\partial x$) along section S3 (see Figure 1 for station locations). The cutoff frequency $\omega_c = 0.81$ cpy (cutoff period $T_c = 450$ day) is marked in grey dashed lines in Figures A1d–A1f. The abbreviation cpy stands for cycles per year.

leakage from the seasonal into the interannual band, the running mean and pl66tn filters cut the seasonal power down by a factor of 10, significantly reducing contamination in the interannual band of our interest (2.5–7 years). However, the pl66tn filter appears to provide smoother results and damp more high-frequency power, because it applies a wider weight function in the time domain (wider than four times the cutoff period). As such, the pl66tn filter prevents its use on the shorter time series (e.g., the 3 year current meter series). The running mean filter slightly attenuates the low-frequency power, but the power in the interannual band is well preserved. For the annual anomalies of the deseasoned data, the long-term mean seasonal cycle is removed, and the anomalies are averaged in annual time bins. This method produces similar results to the other two filters, but considerable loss of temporal resolution makes it too short for spectral analysis.

Results of the correlation analyses are summarized in Table A1, and the reported correlation coefficients are quantitatively similar across the three filters. Although the 450 day running mean filter shows some limitations, allowing slight leakage at seasonal periods and attenuation at longer periods, the contamination is negligible relative to the magnitude of observed interannual changes in the alongshore winds, along-shelf sea level differences, and cross-shelf seas level slopes. We conclude from these comparisons that, in terms

Table A1. The Comparison of Correlation Coefficients (Spearman's Type) Calculated for Low-Pass Filtered Alongshore Wind Stress (τ_y), Along-Shelf Sea Level Differences ($\Delta\eta_y$), and Cross-Shelf Sea Level Slopes ($\partial\eta/\partial x$)

		Correlation Analyses		
Stations		450 Day Running Mean (n = 660, monthly)	450 Day pl66tn (n = 660, monthly)	Annual Anomalies of Deseasoned Data (n = 55, yearly)
τ_y				
Sydney	Sable Island	0.51	0.61	0.63
$\Delta\eta_y$		(n = 660, monthly)	(n = 660, monthly)	(n = 55, yearly)
Halifax	Boston	0.85	0.84	0.86
Yarmouth	Halifax	0.68[a]	0.71[a]	0.64[a]
Boston	Yarmouth	0.74[a]	0.76[a]	0.70[a]
τ_y and $\Delta\eta_y$		(n = 660, monthly)	(n = 660, monthly)	(n = 55, yearly)
Sydney	Halifax	0.44	0.44	0.48
Sydney	Yarmouth	0.58[a]	0.50[a]	0.55[a]
Sydney	Boston	0.36	0.36	0.34
Sable Island	Halifax	0.11	0.21	0.18 ($p = 0.18$)
Sable Island	Yarmouth	0.44[a]	0.42[a]	0.37[a]
Sable Island	Boston	0.29	0.37	0.30
τ_y and $\partial\eta/\partial x$		(n = 854, weekly)	(n = 854, weekly)	(n = 17, yearly)
Sydney	S3	0.46	0.36	0.53
Sydney	S2	0.64	0.59	0.61
Sydney	S1	0.73	0.72	0.70
Sable Island	S3	0.43	0.22	0.39 ($p = 0.12$)
Sable Island	S2	0.54	0.46	0.52
Sable Island	S1	0.67	0.54	0.65

In order to remove seasonal or higher frequency fluctuations, a low-pass filter was applied to all the data prior to correlation calculation. Comparison was done to test three different filters: running mean, pl66tn, and annual anomalies of deseasoned data. The cutoff period was set to 450 day for the first two filters. Correlation coefficients are divided into four categories. For each category, the number of records (n) and temporal resolution were given. All the correlation coefficients are significant at $p < 0.01$ unless marked otherwise

[a]Shorter time series than the others in the category, n = 544.

[b]Shorter time series than the others in the category, n = 46.

of the frequency characteristics of the data set and the analyses performed, the 450 day running mean filter is efficient in eliminating seasonal and higher frequency signals and thus appropriate for low-pass filtering time records prior to correlations analyses. Yet it should be noted that each filtering method presented above has its advantages and disadvantages, so the choice of the "appropriate" one is in the context of this particular data set and study goal.

Acknowledgments

This work was supported by NOAA's Fisheries and the Environment Program, Grant #12-03 and through NOAA Cooperative Agreement NA09OAR4320129. RJ worked on this paper as a CINAR (Cooperative Institute for the North Atlantic Region) Fellow. We thank Steven Lentz for useful discussion on analyzing the observations and Peter Smith for providing current meter observations at station C2. We also thank Pengfei Lin who assisted initial data processing as a guest investigator in RJ's lab. We are grateful to three anonymous reviewers for their valuable comments that have improved our manuscript.

References

Beardsley, R. C., and L. K. Rosenfeld (1983), Introduction to the CODE-1 moored array and large-scale data report, in *CODE-1: Moored Array and Large-Scale Data Report*, edited by L. K. Rosenfeld, *Tech. Rep. WHOI-83-23, CODE Tech. Rep. 21*, pp. 1−16, Woods Hole Oceanogr. Inst., Woods Hole, Mass.

Benada, R. (1997), Merged GDR (TOPEX/Poseidon) users handbook, in *Rep. JPL D-11007*, p. 124, Jet Propul. Lab., Pasadena, Calif.

Brown, W., and J. Irish (1993), The annual variation of water mass structure in the Gulf of Maine: 1986–1987, *J. Mar. Res.*, *51*(1), 53–107.

Chapman, D. C., and R. C. Beardsley (1989), On the origin of shelf water in the Middle Atlantic Bight, *J. Phys. Oceanogr.*, *19*(3), 384–391, doi:10.1175/1520-0485(1989)019<0384:OTOOSW>2.0.CO;2.

Chapman, D. C., J. A. Barth, R. C. Beardsley, and R. G. Fairbanks (1986), On the continuity of mean flow between the Scotian Shelf and the Middle Atlantic Bight, *J. Phys. Oceanogr.*, *16*(4), 758–772, doi:10.1175/1520-0485(1986)016<0758:OTCOMF>2.0.CO;2.

Csanady, G. (1982), *Circulation in the Coastal Ocean*, D. Reidel, Dordrecht, Netherlands.

Deese-Riordan, H. E. (2009), Salinity and stratification in the Gulf of Maine: 2001–2008, Open-access dissertation thesis, 194 p., Univ. of Maine, Maine.

Drinkwater, K., and D. Gilbert (2004), Hydrographic variability in the waters of the Gulf of St. Lawrence, the Scotian Shelf and the eastern Gulf of Maine (NAFO Subarea 4) during 1991–2000, *J. Northwest Atl. Fish. Sci.*, *34*, 85.

Greenberg, D. A., J. W. Loder, Y. Shen, D. R. Lynch, and C. E. Naimie (1997), Spatial and temporal structure of the barotropic response of the Scotian Shelf and Gulf of Maine to surface wind stress: A model-based study, *J. Geophys. Res.*, *102*(C9), 20,897–20,915, doi:10.1029/97JC00442.

Greene, C. H., and A. J. Pershing (2007), Climate drives sea change, *Science*, *315*(5815), 1084–1085.

Greene, C. H., B. C. Monger, L. P. McGarry, M. D. Connelly, N. R. Schnepf, A. J. Pershing, I. M. Belkin, P. S. Fratantoni, D. G. Mountain, and R. S. Pickart (2012), Recent arctic climate change and its remote forcing of Northwest Atlantic Shelf ecosystems, *Oceanography*, *25*(3), 208–213, doi:10.5670/oceanog.2012.64.

Häkkinen, S. (2002), Freshening of the Labrador Sea surface waters in the 1990s: Another great salinity anomaly?, *Geophys. Res. Lett.*, *29*(24), 2232, doi:10.1029/2002GL015243.

Hameed, S., and S. Piontkovski (2004), The dominant influence of the Icelandic Low on the position of the Gulf Stream northwall, *Geophys. Res. Lett.*, *31*, L09303, doi:10.1029/2004GL019561.

Han, G. (2002), Interannual sea-level variations in the Scotia-Maine region in the 1990s, *Can. J. Remote Sens.*, *28*(4), 581–587.

Han, G., C. Tang, and P. Smith (2002), Annual variations of sea surface elevation and currents over the Scotian Shelf and slope, *J. Phys. Oceanogr.*, *32*(6), 1794–1810.
Hannah, C. G., J. A. Shore, J. W. Loder, and C. E. Naimie (2001), Seasonal circulation on the western and central Scotian Shelf, *J. Phys. Oceanogr.*, *31*(2), 591–615.
Hare, J. A., and J. Kane (2012), Zooplankton of the Gulf of Maine—A changing perspective, *Am. Fish. Soc. Symp.*, *79*, 115–137.
Houghton, R., and R. Fairbanks (2001), Water sources for Georges Bank, *Deep Sea Res., Part II*, *48*(1), 95–114, doi:10.1016/S0967-0645(00)00082-5.
Hurrell, J. W., Y. Kushnir, G. Ottersen, and M. Visbeck (2003), *The North Atlantic Oscillation: Climatic Significance and Environmental Impact, Geophys. Monogr. Ser.*, An overview of the North Atlantic oscillation, J. W. Hurrell, Y. Kushnir, G. Ottersen, M. Visbeck, and M.H. Visbeck, eds, pp. 1–35. vol. 134, AGU, Washington, D. C. [Available at: http://opensky.library.ucar.edu/collections/OSGC-000-000-001-392.]
Hurrell, J. W., and National Center for Atmospheric Research Staff (Eds.) (2013), The Climate Data Guide: Hurrell North Atlantic Oscillation (NAO) Index (PC-based), Natl. Cent. for Atmos. Res., Boulder, Colo. [Available at: https://climatedataguide.ucar.edu/climate-data/hurrell-north-atlantic-oscillation-nao-index-pc-based.]
Ji, R., C. S. Davis, C. Chen, D. W. Townsend, D. G. Mountain, and R. C. Beardsley (2007), Influence of ocean freshening on shelf phytoplankton dynamics, *Geophys. Res. Lett.*, *34*, L24607, doi:10.1029/2007GL032010.
Ji, R., C. S. Davis, C. Chen, D. W. Townsend, D. G. Mountain, and R. C. Beardsley (2008), Modeling the influence of low-salinity water inflow on winter-spring phytoplankton dynamics in the Nova Scotian Shelf–Gulf of Maine region, *J. Plankton Res.*, *30*(12), 1399–1416.
Joyce, T. M. (2002), One hundred plus years of wintertime climate variability in the eastern United States, *J. Clim.*, *15*(9), 1076–1086.
Joyce, T. M., C. Deser, and M. A. Spall (2000), The relation between decadal variability of subtropical mode water and the North Atlantic oscillation, *J. Clim.*, *13*(14), 2550–2569.
Kalnay, E., M. Kanamitsu, R. Kistler, W. Collins, D. Deaven, L. Gandin, M. Iredell, S. Saha, G. White, and J. Woollen (1996), The NCEP/NCAR 40-year reanalysis project, *Bull. Am. Meteorol. Soc.*, *77*(3), 437–471.
Loder, J. W., G. Han, C. G. Hannah, D. A. Greenberg, and P. C. Smith (1997), Hydrography and baroclinic circulation in the Scotian Shelf region: Winter versus summer, *Can. J. Fish. Aquat. Sci.*, *54*(S1), 40–56.
Loder, J. W., W. C. Boicourt, and J. H. Simpson (1998a), Overview of western ocean boundary shelves, in *The Global Coastal Ocean: Regional Studies and Synthesis. The Sea*, vol. 11, edited by A. R. Robinson and K. H. Brink, chap. 1, pp. 3–27, John Wiley, New York.
Loder, J. W., B. Petrie, and G. Gawarkiewicz (1998b), The coastal ocean off northeastern North America: A large-scale view, in *The Global Coastal Ocean: Regional Studies and Synthesis. The Sea*, vol. 11, edited by A. R. Robinson and K. H. Brink, pp. 105–133, John Wiley, New York.
Loder, J. W., J. A. Shore, C. G. Hannah, and B. D. Petrie (2001), Decadal-scale hydrographic and circulation variability in the Scotia–Maine region, *Deep Sea Res., Part II*, *48*(1), 3–35.
Manning, J., and G. Strout (2001), Georges Bank winds: 1975–1997, *Deep Sea Res., Part II*, *48*(1), 115–135.
Mountain, D. G. (2004), Variability of the water properties in NAFO subareas 5 and 6 during the 1990s, *J. Northwest Atl. Fish. Sci.*, *34*, 103.
Noble, M., and B. Butman (1979), Low-frequency wind-induced sea level oscillations along the east coast of North America, *J. Geophys. Res.*, *84*(C6), 3227–3236, doi:10.1029/JC084iC06p03227.
Noble, M., B. Butman, and E. Williams (1983), On the longshelf structure and dynamics of subtidal currents on the eastern United States continental shelf, *J. Phys. Oceanogr.*, *13*(12), 2125–2147.
Petrie, B., and K. Drinkwater (1993), Temperature and salinity variability on the Scotian Shelf and in the Gulf of Maine 1945–1990, *J. Geophys. Res.*, *98*(C11), 20,079–20,089, doi:10.1029/93JC02191.
Petrie, B., and P. C. Smith (1977), Low frequency motions on the Scotian shelf and slope, *Atmosphere*, *15*(3), 117–140.
Petrie, B., K. Drinkwater, D. Gregory, R. Pettipas, and A. Sandström (1996a), Temperature and salinity atlas for the Scotian Shelf and the Gulf of Maine, *Can. Tech. Rep. Hydrogr. Ocean Sci.*, *171*, 398.
Petrie, B., K. Drinkwater, A. Sandström, R. Pettipas, D. Gregory, D. Gilbert, and P. Sekhon (1996b), Temperature, salinity and sigma-t atlas for the Gulf of St. Lawrence, *Can. Tech. Rep. Hydrogr. Ocean Sci.*, *178*, 256.
Ponte, R. M. (2006), Low-frequency sea level variability and the inverted barometer effect, *J. Atmos. Oceanic Technol.*, *23*(4), 619–629.
Sandstrom, H. (1980), On the wind-induced sea level changes on the Scotian Shelf, *J. Geophys. Res.*, *85*(C1), 461–468.
Schwing, F. B. (1989), Subtidal response of the Scotian Shelf bottom pressure field to meteorological forcing, *Atmos. Ocean*, *27*(1), 157–180.
Schwing, F. B. (1992a), Subtidal response of Scotian Shelf circulation to local and remote forcing. I: Observations, *J. Phys. Oceanogr.*, *22*(5), 523–541.
Schwing, F. B. (1992b), Subtidal response of Scotian Shelf circulation to local and remote forcing. II: Barotropic model, *J. Phys. Oceanogr.*, *22*(5), 542–563.
Smith, P. C. (1983), The mean and seasonal circulation off southwest Nova Scotia, *J. Phys. Oceanogr.*, *13*(6), 1034–1054.
Smith, P. C. (1989), Seasonal and interannual variability of current, temperature and salinity off southwest Nova Scotia, *Can. J. Fish. Aquat. Sci.*, *46*(S1), 4–20.
Smith, P. C., R. W. Houghton, R. G. Fairbanks, and D. G. Mountain (2001), Interannual variability of boundary fluxes and water mass properties in the Gulf of Maine and on Georges Bank: 1993–1997, *Deep Sea Res., Part II*, *48*(1), 37–70.
Smith, P. C., N. R. Pettigrew, P. Yeats, D. W. Townsend, and G. Han (2012), Regime shift in the Gulf of Maine, in *Advancing an Ecosystem Approach in the Gulf of Maine, American Fisheries Society Symposium*, edited by R. L. Stephenson et al., pp. 185–203, Bethesda, Md.
Smith, S. D. (1980), Wind stress and heat flux over the ocean in gale force winds, *J. Phys. Oceanogr.*, *10*, 709–726.
Taylor, A., and J. Stephens (1980), Latitudinal displacements of the gulf-stream (1966 to 1977) and their relation to changes in temperature and zooplankton abundance in the NE Atlantic, *Oceanol. Acta*, *3*(2), 145–149.
Taylor, A. H., and J. A. Stephens (1998), The North Atlantic oscillation and the latitude of the Gulf Stream, *Tellus, Ser. A*, *50*(1), 134–142.
Thompson, K. R. (1986), North Atlantic sea level and circulation, *Geophys. J. R. Astron. Soc.*, *87*(1), 15–32.
Townsend, D. W., N. D. Rebuck, M. A. Thomas, L. Karp-Boss, and R. M. Gettings (2010), A changing nutrient regime in the Gulf of Maine, *Cont. Shelf Res.*, *30*(7), 820–832.
Woodworth, P., and R. Player (2003), The permanent service for mean sea level: An update to the 21st century, *J. Coastal Res.*, *19*, 287–295.